JVI Journals.ASM.org

Targeting Importin-α7 as a Therapeutic Approach against Pandemic Influenza Viruses

Patricia Resa-Infante,[a] Duncan Paterson,[b] Jaume Bonet,[c]* Anna Otte,[a]* Baldo Oliva,[c] Ervin Fodor,[b] Gülsah Gabriel[a,d]

Heinrich Pette Institute, Leibniz Institute for Experimental Virology, Hamburg, Germany[a]; Sir William Dunn School of Pathology, University of Oxford, Oxford, United Kingdom[b]; Structural Bioinformatics Laboratory (GRIB), Universitat Pompeu Fabra, Barcelona Research Park of Biomedicine (PRBB), Barcelona, Spain[c]; Center for Cellular and Structural Biology in Medicine, University of Lübeck, Lübeck, Germany[d]

ABSTRACT

Viral drug resistance is believed to be less likely to occur if compounds are directed against cellular rather than viral proteins. In this study, we analyzed the feasibility of a crucial viral replication factor, namely, importin-α7, as a cellular drug target to combat pandemic influenza viruses. Surprisingly, only five viral lung-to-lung passages were required to achieve 100% lethality in importin-α7$^{-/-}$ mice that otherwise are resistant. Viral escape from importin-α7 requirement was mediated by five mutations in the viral ribonucleoprotein complex and the surface glycoproteins. Moreover, the importin-α7$^{-/-}$ mouse-adapted strain became even more virulent for wild-type mice than the parental strain. These studies show that targeting host proteins may still result in viral escape by alternative pathways, eventually giving rise to even more virulent virus strains. Thus, therapeutic intervention strategies should consider a multitarget approach to reduce viral drug resistance.

IMPORTANCE

Here, we investigated the long-standing hypothesis based on *in vitro* studies that viral drug resistance occurrence is less likely if compounds are directed against cellular rather than viral proteins. Here, we challenged this hypothesis by analyzing, in an *in vivo* animal model, the feasibility of targeting the cellular factor importin-α7, which is crucial for human influenza virus replication and pathogenesis, as an efficient antiviral strategy against pandemic influenza viruses. In summary, our studies suggest that resistance against cellular factors is possible *in vivo*, and the emergence of even more virulent viral escape variants calls for particular caution. Thus, therapeutic intervention strategies should consider a multitarget approach using compounds against viral as well as cellular factors to reduce the risk of viral drug resistance and potentially increased virulence.

Influenza A viruses are responsible for acute respiratory diseases in humans posing a severe burden for health and economy worldwide. Vaccination is considered the best option for disease prophylaxis. However, production of novel vaccines in the case of a pandemic requires at least 6 months. Thus, antiviral drugs are essential to bridge this gap. Two classes of antiviral agents currently are available against influenza virus: neuraminidase inhibitors and adamantanes (1). However, their efficiency is limited, and several influenza virus strains have developed resistance to these virus-directed drugs (2). Hence, development of novel antiviral agents is urgently required.

Inhibitors developed against host cell proteins are considered an attractive strategy compared to drugs that target viral proteins, because they are less prone to mutations than viral proteins. Thus, it is believed that targeting host factors would limit the emergence of drug-resistant virus strains. Several compounds targeting cellular factors to halt influenza virus replication currently are under development (3–5). For example, inhibitors targeting the Raf/MEK/ERK signaling pathway, NF-κB signaling, the phosphatidylinositol 3-kinase/Akt pathway, and the protein kinase C signaling cascade are already in an early phase of preclinical development (6).

For influenza virus, the nuclear import protein importin-α7 is a crucial pathogenicity factor that increases human-type influenza virus replication by an unknown mechanism beyond nuclear import. Mice with a deleted importin-α7 gene (α7$^{-/-}$) are resistant to an otherwise lethal 2009 pandemic H1N1 influenza virus infection (7–9). Since deletion of the importin-α7 gene did not cause an obvious phenotype in adult α7$^{-/-}$ mice (10), its transient inhibition poses a very attractive target to combat human-type influenza viruses.

In this study, we investigated whether targeting importin-α7 would provide an efficient antiviral strategy against pandemic influenza viruses, reducing the risk of viral resistance. In particular, we employed a method of accelerated viral evolution, thereby challenging viral escape in a resistant host.

MATERIALS AND METHODS

Ethical statement. All animal experiments were approved by the relevant German authority (Behörde für Gesundheit und Verbraucherschutz, Hamburg, Germany) and performed according to the national guidelines of the animal protection law (Tierschutzgesetz; project number 97/11) in Germany.

Received 6 March 2015 **Accepted** 10 June 2015

Accepted manuscript posted online 17 June 2015

Citation Resa-Infante P, Paterson D, Bonet J, Otte A, Oliva B, Fodor E, Gabriel G. 2015. Targeting importin-α7 as a therapeutic approach against pandemic influenza viruses. J Virol 89:9010–9020. doi:10.1128/JVI.00583-15.

Editor: B. Williams

Address correspondence to Gülsah Gabriel, guelsah.gabriel@hpi.uni-hamburg.de.

* Present address: Jaume Bonet, Laboratory of Protein Design & Immunoengineering, STI, EPFL, Lausanne, Switzerland; Anna Otte, Institute of Biochemistry, Kiel University, Kiel, Germany.

doi:10.1128/JVI.00583-15

Animal experiments. Importin-$\alpha7^{-/-}$ ($\alpha7^{-/-}$) mice (8, 10) and wild-type (WT) littermates in the C57BL/6J genetic background were bred and housed under specific-pathogen-free conditions at the animal facility of the Heinrich-Pette-Institute, Leibniz Institute for Experimental Virology, Hamburg, Germany.

Mice were anesthetized with ketamine/xylazine (70 mg/kg of body weight and 7 mg/kg, respectively) and inoculated intranasally with 50 μl of virus diluted in phosphate-buffered saline (PBS). Survival and weight loss were monitored for 14 days. The 50% mouse lethal dose (MLD_{50}) was determined using serial 10-fold virus dilutions (11). Mice were humanely euthanized upon >25% weight loss.

Cells. Madin-Darby canine kidney (MDCK) cells were grown in minimal essential medium (PAA, Austria) supplemented with fetal calf serum (FCS; PAA, Austria), L-glutamine (PAA, Austria), and penicillin-streptomycin (PAA, Austria). Human embryonic kidney 293T (HEK) and human alveolar adenocarcinoma (A549) cells were grown in DMEM (Dulbecco's modified Eagle's medium; PAA, Austria) supplemented with 10% FCS, L-glutamine, and penicillin-streptomycin. WT and $\alpha7^{-/-}$ murine embryonic fibroblasts (MEF) were grown in DMEM supplemented with 10% FCS, penicillin-streptomycin, L-glutamine, nonessential amino acids (PAA, Austria) and sodium pyruvate (PAA, Austria). MEFs were kindly provided by M. Bader (Max Delbrück Center for Molecular Medicine, Berlin, Germany) (12).

HEK and A549 cells were transduced with lentiviral vectors expressing short hairpin RNA (shRNA) anti-importin-α7 (clone identifier NM_012316.3-223s1c1; Sigma-Aldrich, Germany) to generate importin-α7 knockdown cell lines, named HEK-shα7 and A549-shα7. Transduced cells were selected and maintained in medium containing 2 μg/ml puromycin (Calbiochem, USA). shRNA-mediated knockdown was confirmed by Western blotting using anti-importin-α5/α7 antibody (kindly provided by the E. Hartmann Institute of Biology, Lübeck, Germany) (8). Glyceraldehyde-3-phosphate dehydrogenase (GAPDH) expression was detected by an anti-GAPDH antibody (Cell Signaling Technology, Inc., USA).

Adaptation of pH1N1 influenza virus to importin-$\alpha7^{-/-}$ mice. We used the 2009 pandemic H1N1 A/Hamburg/NY1580/09 virus strain (abbreviated as pH1N1) as a parental strain (8, 13, 14). Three $\alpha7^{-/-}$ mice were intranasally infected with 10^5 PFU of the pH1N1 strain. Lungs were harvested and homogenized 3 days postinfection (p.i.). Subsequently, 50 μl of the pooled lung homogenate supernatant was used to intranasally infect the next group of three $\alpha7^{-/-}$ mice. Serial passaging was stopped upon 100% lethality. One viral clone was isolated from the lung homogenates of the fifth passage by plaque purification from MDCK cells and named pH1N1-MA7. All experiments were performed at the biosafety level 2 facilities of the Heinrich-Pette-Institute, Leibniz Institute for Experimental Virology.

Plasmids and recombinant pH1N1 viruses. The gene segments of pH1N1 and pH1N1-MA7 viruses were sequenced as described previously (15). pH1N1 genes were cloned into the pHW2000 vector to generate recombinant influenza viruses by reverse genetics. pH1N1-MA7 specific mutations were introduced using the QuikChange site-directed mutagenesis kit (Stratagene/Agilent Technologies, USA). Virus stocks were grown in MDCK cells and sequenced for verification.

PB1, PB2, PA, and NP genes from pH1N1 or pH1N1-MA7 viruses additionally were cloned from pHW2000 vector into pcDNA3.1 vector to generate pC-HH15-PB1, pC-HH15-PB2, pC-HH15-PA, pC-HH15-NP, pC-HH15-PA_{MA7}, and pC-HH15-NP_{MA7} expression plasmids.

Polymerase activity. HEK or HEK-shα7 cells were cotransfected with pC-HH15-PB1, pC-HH15-PB2, pC-HH15-PA, pC-HH15-NP, pC-HH15-PA_{MA7}, or pC-HH15-NP_{MA7} to generate recombinant RNPs. Reporter constructs pPol-I-NP-Luc-human (encoding firefly luciferase in negative polarity flanked by the nontranslated regions of influenza NP segment) (16) and pRL-TK (encoding *Renilla* luciferase; Promega, USA) were cotransfected. The transfection solution was prepared by incubating a mixture of DNA, polyethylenimine (PEI; Polysciences), and DMEM in a ratio of 1 μg DNA to 2.4 μg PEI to 600 μl DMEM for 20 min at room temperature. At 20 h posttransfection, luciferase activity was measured with a dual-luciferase reporter assay system (Promega, USA). All experiments were performed in triplicates.

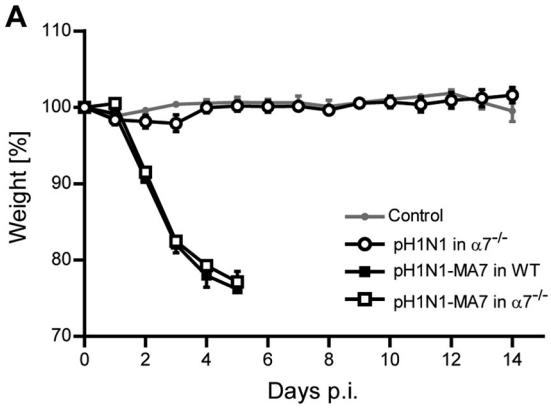

B

MLD_{50} (p.f.u.)	pH1N1	pH1N1-MA7
WT	$10^{3.5}$	$10^{2.4}$
$\alpha7^{-/-}$	$>10^5$	$10^{2.6}$

C

Protein	Adaptive mutations in pH1N1-MA7
PA	Asp 27 Glu
NP	Gly 102 Arg
HA	Lys 171 Glu Asp 239 Gly
NA	Tyr 170 His

FIG 1 Adaptation of 2009 pH1N1 influenza virus to $\alpha7^{-/-}$ mice. (A) Pathogenicity of pH1N1-MA7 influenza virus. WT (black squares) or $\alpha7^{-/-}$ (open squares) mice were intranasally inoculated with 10^5 PFU of pH1N1-MA7 virus. As controls, a group of $\alpha7^{-/-}$ mice were infected with the parental strain 2009 pH1N1 (open circles) or received PBS only (gray circle). Weight loss was monitored for 14 days. Data shown represent means ± SEM ($n = 5$ to 13). (B) MLD_{50} of pH1N1 and pH1N1-MA7 strains in WT and $\alpha7^{-/-}$ mice. (C) Amino acid sequence differences are shown for parental pH1N1 and adapted pH1N1-MA7 viruses.

Coimmunoprecipitation assay. Immunoprecipitations were performed using EZview red anti-FLAG M2 affinity gel (Sigma, USA) and eluted using a 3× FLAG peptide (Sigma, USA) according to the manufacturer's instructions. The quantification of coimmunoprecipitation products was performed by Western blotting using mouse anti-FLAG (Sigma, USA) and rabbit anti-feline panleukemia virus serum (17) antibodies. The β-actin antibody (Abcam, United Kingdom) was used for normalization of the total protein amount used in respective cell lysates. Immunoreactive bands were visualized with the Bioimager Image Quant LAS 4000 at nonsaturated levels and quantified by densitometry with ImageJ software.

Analysis of virus replication. A549 and A549-shα7 cells were infected at a multiplicity of infection (MOI) of 0.1 with pH1N1 or pH1N1-MA7 virus, respectively, in the presence of 0.25 μg/μl L-1-tosylamide-2-phenylethyl chloromethyl ketone (TPCK)-trypsin. Supernatants were collected at 0, 24, 48, and 72 h p.i., and virus titers were determined as plaque-forming units on MDCK cells.

WT and $\alpha7^{-/-}$ MEFs were infected at an MOI of 2 with pH1N1

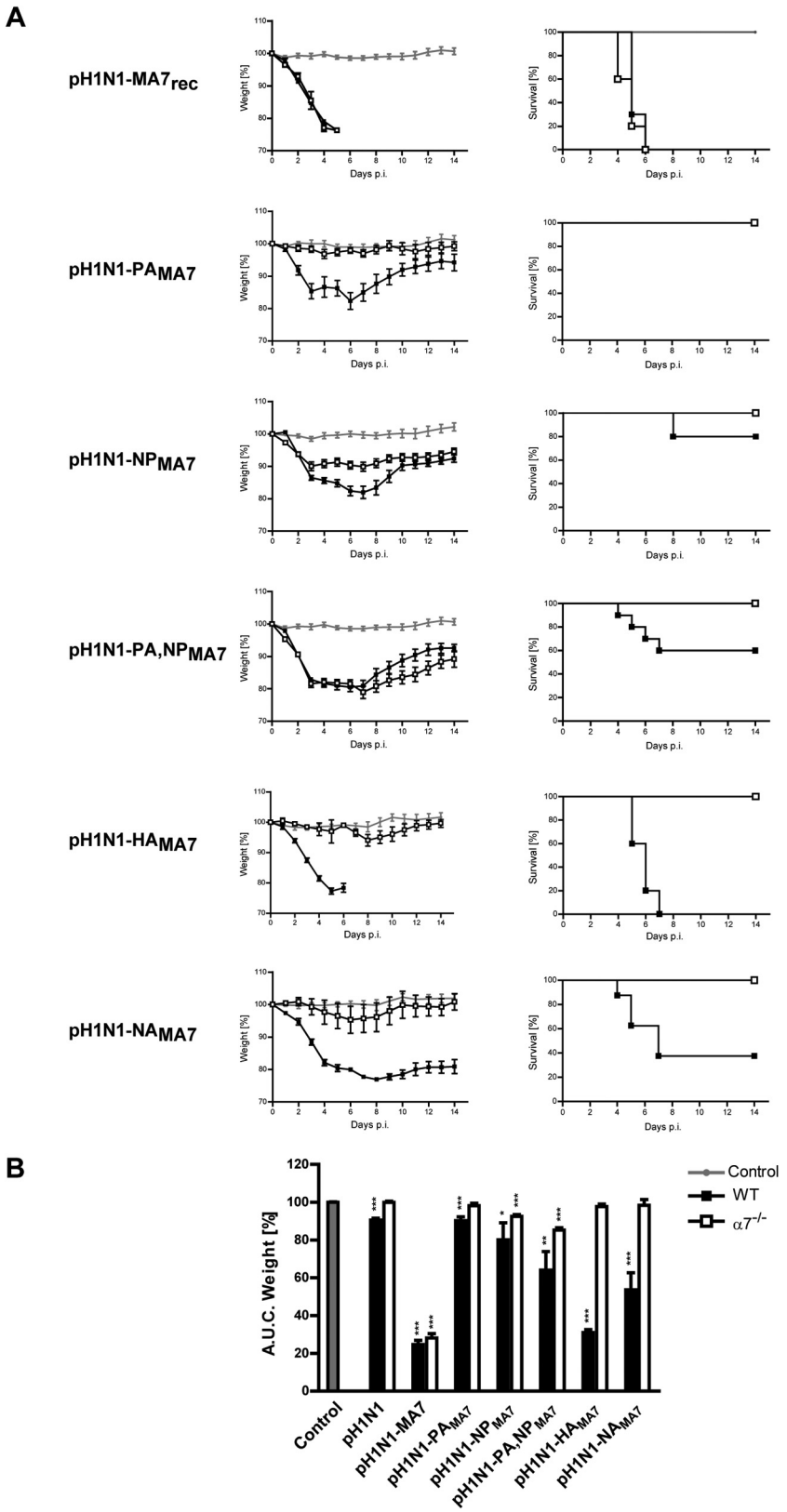

FIG 2 Pathogenicity of pH1N1-MA7 recombinant viruses in WT and $\alpha7^{-/-}$ mice. (A) WT (black square) or $\alpha7^{-/-}$ (open square) mice were intranasally inoculated with recombinant viruses, i.e., 10^4 PFU of adapted pH1N1-MA7$_{rec}$, 10^5 PFU of pH1N1-PA$_{MA7}$, 10^5 PFU of pH1N1-NP$_{MA7}$, 10^5 PFU of pH1N1-PA,NP$_{MA7}$, 10^5 PFU of pH1N1-HA$_{MA7}$, and 10^5 PFU of pH1N1-NA$_{MA7}$. Weight loss and survival was monitored for 14 days. Control mice received PBS only (gray circle). Data shown represent means ± SEM ($n = 5$ to 15). (B) Weight loss has been summarized as representing the mean area under the curve (AUC). WT (black bars) or $\alpha7^{-/-}$ (white bars) mice were infected with 10^5 PFU of wild-type viruses (pH1N1 and pH1N1-MA7) and recombinant viruses (pH1N1-PA$_{MA7}$, pH1N1-NP$_{MA7}$, pH1N1-PA,NP$_{MA7}$, pH1N1-HA$_{MA7}$, and pH1N1-NA$_{MA7}$). Control mice received PBS (gray bar). Data shown represent means ± SEM ($n = 5$ to 15; $P < 0.05$ [*], $P < 0.01$ [**], and $P < 0.001$ [***], all by Student's t test compared to the control group).

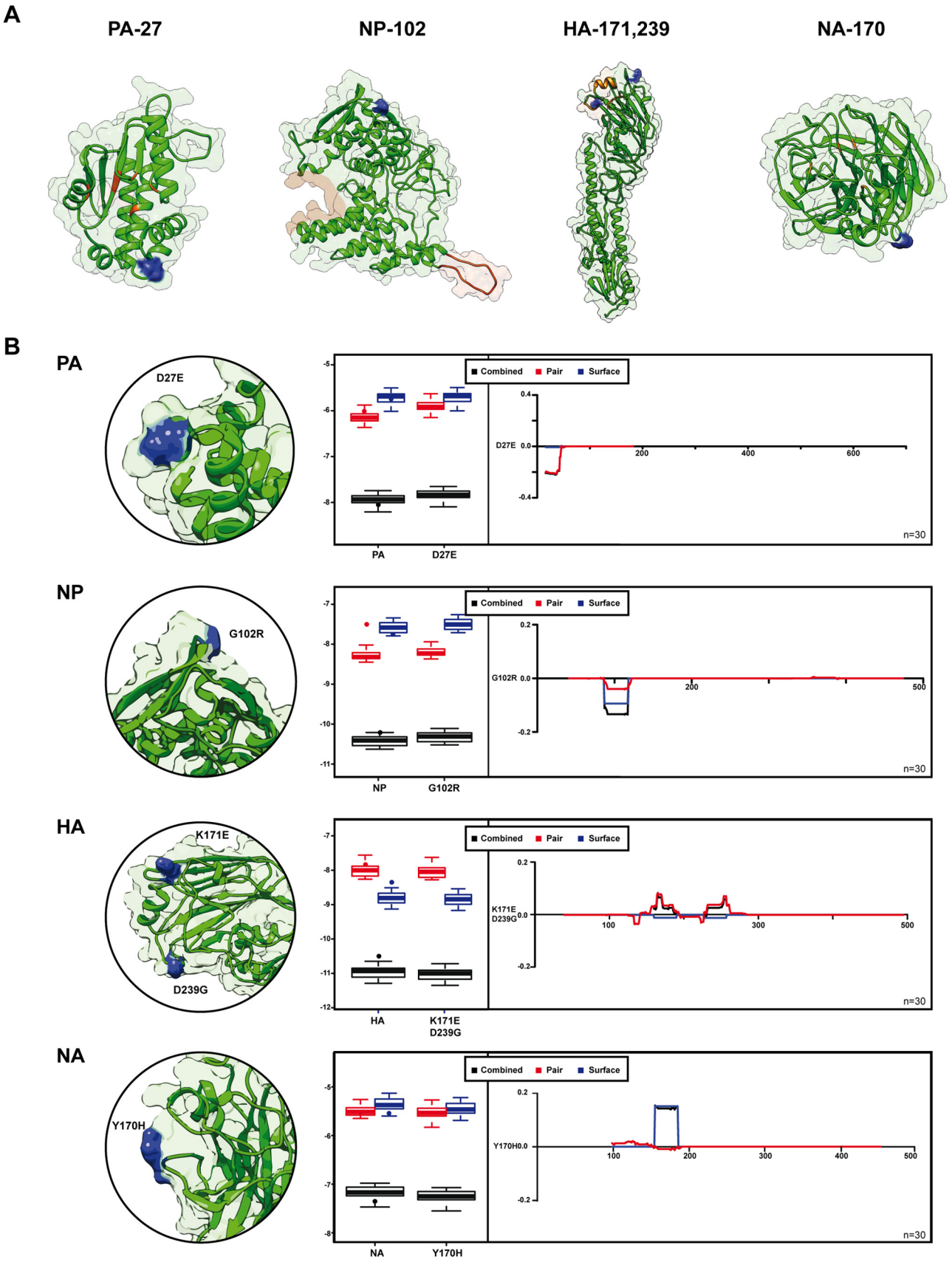
A
PA-27
NP-102
HA-171,239
NA-170
B
PA
D27E
Combined
Pair
Surface
PA
D27E
n=30
NP
G102R
NP
G102R
n=30
HA
K171E
D239G
HA
K171E
D239G
n=30
NA
Y170H
NA
Y170H
n=30

recombinant viruses containing pH1N1-MA7 mutations as indicated. Total RNA was isolated at 24 h p.i. by extraction with TRIzol reagent (Invitrogen, USA). Viral RNA accumulation was analyzed by primer extension using specific primers for the viral NP gene (18). Primer PrE-NP− (5′-ATGATGGAAAGTGCAAAGCC-3′) was used to detect vRNA and primer PrE-NP+ (5′-ATTTCTGTGGCATCCTGGC-3′) to detect cRNA and mRNA. A primer detecting cellular 5S rRNA (5′-TCCCAGGCGGT CTCCCATCC-3′) was used for normalization. Transcription products were analyzed on 6% polyacrylamide gels containing 7 M urea in Tris-borate-EDTA (TBE) buffer, detected by autoradiography, and quantified by densitometry of phosphorimages using AIDA software.

Modeling of pH1N1 protein structure domains. The three-dimensional (3D) conformations of the proteins of interest from the parental pH1N1 strain were modeled to evaluate the effects of the mutations over their structural stability. The templates used to build these structures were their closest homologues with known structures in the Protein Data Bank (PDB) (19, 20), found by sequence similarity through BLAST (21). In all cases, a template containing the region with the mutations was found with an *E* value of 0, which indicates the probability of a protein-template assignation due to chance. Specifically, PA was modeled over 4AVL-chainD (22), NP over 4DYS-chainC, NA over 4B7R-chainD (23), and HA over 2WR0-chainB (24). Except for PA, the templates covered more than 80% of the protein length. Thirty parental models were created for each protein through MODELLER (25). Global and local energies were analyzed with Prosa (26). Global energy (z score) represents a normalized score of the stability of the protein. Local energy represents the individual stability of each residue in the structural conditions in a given 3D representation. Both values are further divided in surface, pair (structural), and combined (pair plus surface) energy. As a rule, negative values represent stable conformations. A total of 30 variants for each possible mutant of interest were created with Prosa and analyzed for both their global and local energies.

Statistical analysis. All data shown are presented as means ± standard errors of the means (SEM). Means, SEM, Student's *t* test (unpaired, 2-tailed), and Mantel-Cox test were calculated with Prism GraphPad software (GraphPad Software, Inc., USA). Statistical significance was defined as $P < 0.05$ (*, $P < 0.05$; **, $P < 0.01$; ***, $P < 0.001$).

RESULTS

Adaptation of a 2009 pandemic H1N1 influenza virus strain to importin-α7$^{-/-}$ mice. The importin-α7 gene is crucial for replication and pathogenicity of human-type influenza A viruses in mammals. The lack of the importin-α7 gene leads to 100% survival in mice infected with several 2009 pandemic H1N1 influenza virus strains, whereas 100% of WT mice succumb to infection (8). Here, we addressed whether targeting importin-α7 would pose a promising antiviral strategy to combat human influenza viruses. To analyze whether viral escape would be possible using a cellular target, we challenged this approach by adapting a 2009 pandemic H1N1 strain (A/Hamburg/NY1580/09; pH1N1) to importin-α7$^{-/-}$ (α7$^{-/-}$) mice by serial lung-to-lung passages. Interestingly, 100% lethality could be achieved after only 5 passages. We isolated one α7$^{-/-}$ mouse-adapted virus clone (pH1N1-MA7) by plaque assay and assessed its pathogenesis in WT and α7$^{-/-}$ mice compared to that of its parental strain (Fig. 1A). Consistent with previous findings, infection of α7$^{-/-}$ mice with the parental pH1N1 strain did not result in significant weight loss or lethality (8). However, the adapted pH1N1-MA7 strain was lethal for WT (MLD_{50}, $10^{2.4}$ PFU) and α7$^{-/-}$ mice (MLD_{50}, $10^{2.6}$ PFU). Notably, the pH1N1-MA7 strain was more virulent for WT mice than its non-adapted parental strain, suggesting that its virulence increased during viral escape from importin-α7 requirement (Fig. 1B). Sequencing of both viral genomes revealed two amino acid substitutions in the ribonucleoprotein (RNP) complex (PA D27E and NP G102R) and three substitutions in the viral surface glycoproteins, including two mutations in HA (K171E and D239G) and one mutation in NA (Y170H) (Fig. 1C).

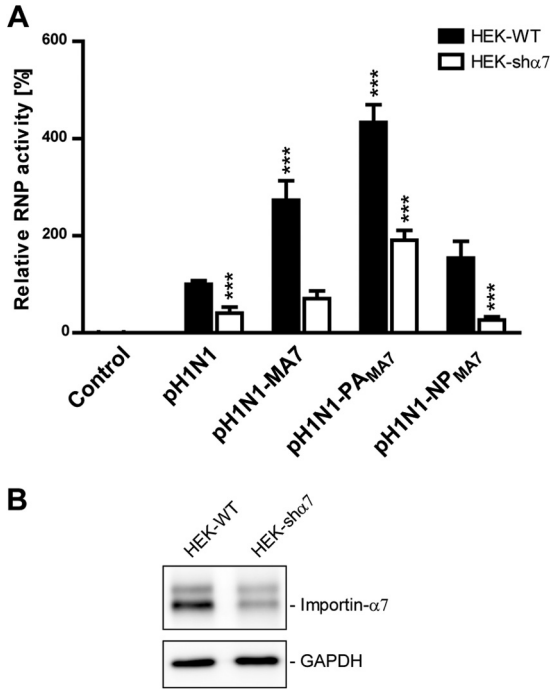

FIG 4 Biological activity of recombinant RNPs with adaptive mutations in epithelial HEK and HEK-shα7 cell lines. (A) Human HEK-WT (black bars) and HEK-shα7 (white bars) cells were cotransfected with plasmids expressing PB1, PA, NP, and PB2, as well as a plasmid encoding *Renilla* luciferase and a plasmid encoding firefly luciferase in negative polarity, flanked by the non-translated regions of influenza NP segment. Plasmid expressing PB1 was omitted as a negative control. Plasmids encoding PA_{MA7} and NP_{MA7} were used when indicated, and both were used in pH1N1-MA7. At 20 h posttransfection, luciferase accumulation was determined. Values were normalized to *Renilla* expression, and the activity of the pH1N1 RNP in HEK-WT cells was set to 100% (means ± SEM; $n = 9$ to 18; ***, $P < 0.001$ by Student's *t* test compared to pH1N1 RNP activity in HEK-WT cells). (B) Confirmation of importin-α7 knockdown in human HEK cells by Western blotting. Since importin-α7 antibody cross-reacts with importin-α5, the doublet represents importin-α5 (upper band) and importin-α7 (lower band). GAPDH was used as a loading control.

FIG 3 Localization of the adaptive mutations in pH1N1 protein structure and their effect on structural stability. (A) Structural models of the regions surrounding the adaptive mutations of pH1N1-MA7 with homologous structures. Adaptive mutations are indicated in blue. Relevant sites in the structures are indicated in orange (PA endonuclease active site, RNA binding site and oligomerization domain of NP, HA receptor binding site, and NA active site). (B) Global z score (as boxplots) and local energy comparison between the mutants of pH1N1-MA7 and their respective wild types (pH1N1). The *x* axis shows the corresponding amino acid position, and the *y* axis shows the energy change. Each set is composed of 30 structural models. Pair (red), surface (blue), and combined (black) energy are shown for each analysis. Dots placed above the z score distributions of the pH1N1 models represent the score of the structural template.

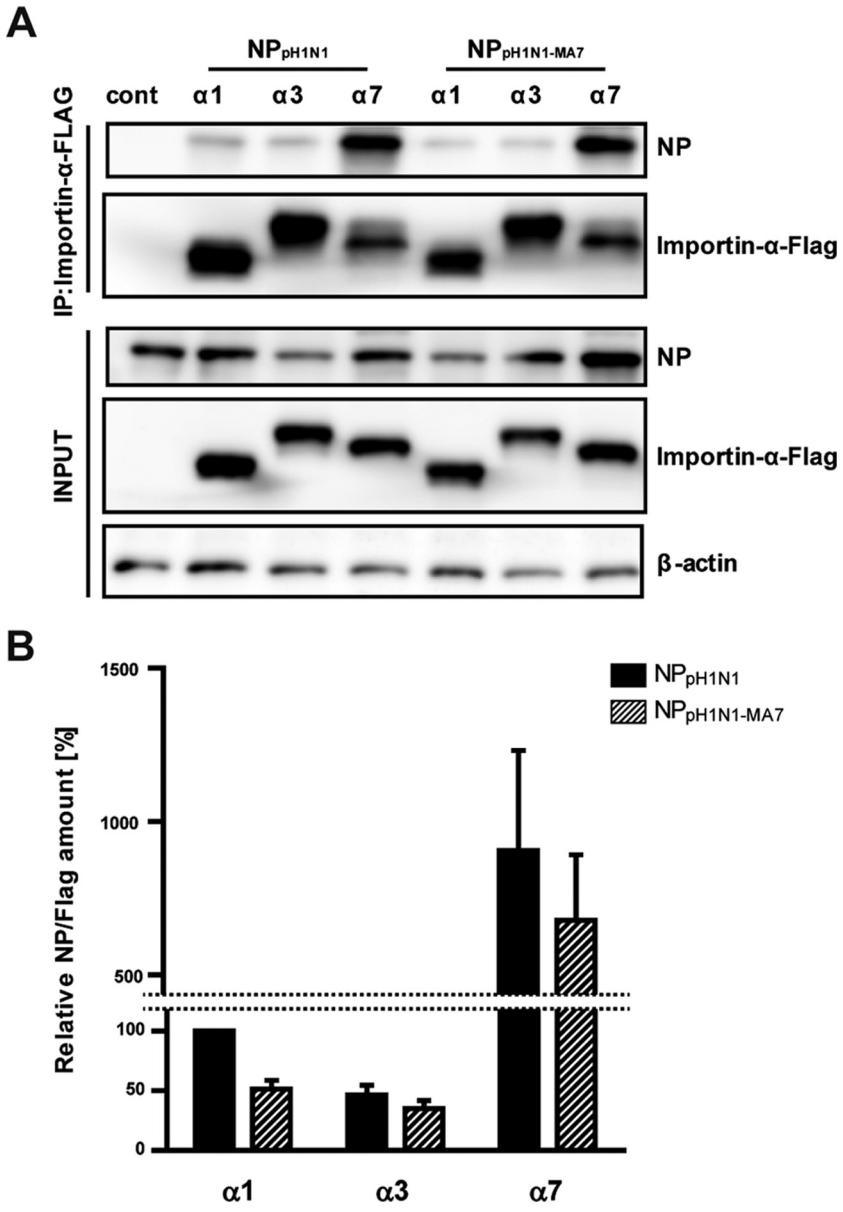

FIG 5 Importin-α binding affinities to NP monomers with adaptive mutation. (A) Human HEK-WT cells were cotransfected with plasmids encoding FLAG-tagged importins (α1, α3, or α7) and NP or NP_{MA7}. NP-only transfected cells served as a control (cont). At 48 h posttransfection, importins were immunoprecipitated using the FLAG tag, and coimmunoprecipitated NP was determined by Western blotting. β-Actin was used as a loading control in the input samples. (B) Quantification of NP (black bars) or NP_{MA7} (dashed bars) binding to overexpressed importins. Values of NP were normalized against precipitated importin-α levels, and the relative amount of NP bound to importin-α1 was set to 100%. Data shown represent means ± SEM ($n = 3$).

Overall, we could show that pH1N1 influenza viruses are able to escape the requirement for importin-α7 by acquiring adaptive mutations in the viral RNP and the surface glycoproteins. This escape rendered the virus even more virulent for WT mice.

Identification of host adaptive sites responsible for overcoming viral restriction in importin-$\alpha7^{-/-}$ mice. In order to identify the relevant viral genes responsible for the evasion of viral restriction in $\alpha7^{-/-}$ mice, we generated single-gene reassortant (SGR) recombinant influenza viruses containing one exchanged gene segment of the pH1N1-MA7 strain in the parental pH1N1 virus background. In order to study the role of the RNP on viral pathogenesis, we also generated the double gene reassortant pH1N1-PA,NP_{MA7} virus that contains PA and NP genes of the pH1N1-MA7 strain.

We then assessed the pathogenic potential of these viruses in WT and $\alpha7^{-/-}$ mice (Fig. 2). Infection with the recombinant pH1N1-MA7 ($pH1N1\text{-}MA7_{rec}$) virus containing all five adaptive mutations showed pathogenesis similar to that of the isolated clone. Interestingly, none of the SGR viruses increased lethality in $\alpha7^{-/-}$ mice. However, pH1N1-NP_{MA7} significantly enhanced weight loss in $\alpha7^{-/-}$ mice, which was further increased when combined with the PA_{MA7} gene segment. This suggests a synergistic effect of PA_{MA7} and NP_{MA7} on viral pathogenesis in $\alpha7^{-/-}$ mice. In contrast, pH1N1-HA_{MA7} and pH1N1-NA_{MA7} SGR vi-

ruses did not cause any significant weight loss in $\alpha7^{-/-}$ mice. Conversely, in WT mice, adaptive mutations in HA and NA strongly enhanced pathogenicity, in contrast to adaptive mutations in the RNP (Fig. 2B).

These data suggest that mutations in the RNP are adaptations to the lack of importin-α7, while mutations in HA and NA seem to represent adaptations to the WT animal. However, a combination of both mutations in the RNP as well as in the glycoproteins is required to completely escape importin-α7-mediated restriction in mice.

Adaptive mutations are localized on the respective protein surface. We then generated structural models to investigate the localization of the pH1N1-MA7 adaptive mutations (Fig. 3). All adaptive mutations are located on the surface of the viral proteins. In particular, the PA_{MA7} D27E mutation is located on the surface of the endonuclease domain. The HA_{MA7} D239G mutation is included in the 220-loop element of the receptor binding site, and the HA_{MA7} K171E mutation is near this domain. NP_{MA7} G102R and NA_{MA7} Y170H mutations are located in domains without a specific function described at the moment (Fig. 3A).

To evaluate potential energy changes, we mimicked the adaptive mutations and compared the energies of the different mutants against their parental proteins (Fig. 3B). The comparison showed no significant differences between the parental and the mutant structures in either global (z score) or in local energies. This suggests that these adaptive mutations do not alter the global stability of the protein. Although some local differences are observed, those are extremely small and focused in the surface energy. These results indicate that these mutations in PA, NP, HA, and NA do not directly affect protein conformation, but they might affect interaction with other viral and/or host factors which affect protein functions.

Adaptive mutations increase RNP activity. To study the effect of the adaptive mutations in PA and NP genes on viral polymerase activity, we reconstituted viral RNPs in wild-type (HEK-WT) as well as in importin-α7 knockdown (HEK-shα7) cell lines (Fig. 4). The pH1N1-MA7 polymerase activity was increased up to 3-fold compared to that of the nonadapted pH1N1 polymerase in HEK-WT cells. Interestingly, PA_{MA7} was mainly responsible for this increase in viral polymerase activity in HEK-WT cells, while NP_{MA7} did not show significant effects. However, both pH1N1 and pH1N1-MA7 polymerase activity was restricted in HEK-shα7 compared to that of HEK-WT cells. Similarly, PA_{MA7} was the main mediator of elevated polymerase activity in HEK-shα7 cells.

We next addressed whether the adaptive mutation in NP_{MA7} resulted in altered importin-α binding affecting vRNP activity. NP_{MA7} shows a generally reduced binding affinity to importin-α1, -α3, and -α7 isoforms, which are relevant for influenza virus replication (8), compared to that to nonadapted NP, albeit at a statistically nonsignificant level (Fig. 5).

These findings show that $\alpha7^{-/-}$ adaptive mutations in the RNP mediate partial escape from importin-α7 depletion in mice. However, a complete circumvention of the RNP from importin-α7 requirement could not be achieved. These data suggest that alternative pathways are utilized to circumvent the lack of importin-α7.

Adaptive mutations increase virus replication. We next analyzed the viral replication kinetics of pH1N1-MA7 compared to those of the parental pH1N1 virus in WT epithelial (A549-WT) and in importin-α7 knockdown (A549-shα7) cell lines (Fig. 6).

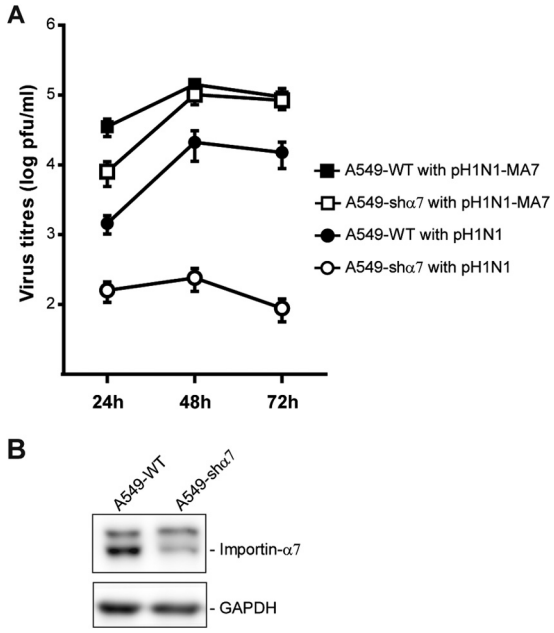

FIG 6 Replication kinetics in epithelial A549 and A549-shα7 cell lines infected with pH1N1-MA7 virus. (A) Human A549-WT and A549-shα7 cells were infected at an MOI of 0.1 with parental (pH1N1) or adapted (pH1N1-MA7) viruses. Virus titers of the supernatants were measured by plaque assay at the indicated hours p.i. Data are expressed as means ± SEM of viral titers ($n = 8$ to 12). (B) Confirmation of importin-α7 knockdown in human A549 cells by Western blotting. Since importin-α7 antibody cross-reacts with importin-α5, the doublet represents importin-α5 (upper band) and importin-α7 (lower band). GAPDH was used as a loading control.

Consistent with previous reports, parental pH1N1 virus replication was strongly impaired in A549-shα7 cells by approximately 2 logs compared to A549-WT cells. In contrast, pH1N1-MA7 virus replication was only slightly reduced in A549-shα7 compared to that in WT cells.

Compared to the pH1N1 parental strain, pH1N1-MA7 mutations remarkably enhanced virus replication in both cell lines, by about 1 log in parental cells (A549-WT) and 3 logs in importin-α7 knockdown cell lines (A549-shα7). However, both parental pH1N1 and adapted pH1N1-MA7 viruses replicated better when importin-α7 expression was not depleted. This suggests that alternative strategies are exploited to overcome the importin-α7 requirement to restore viral replication efficiency in human cells.

Importin-α7 dependency remains upon adaptation. We then investigated the effect of these adaptive mutations on virus replication in cells where the entire importin-α7 gene is deleted in order to abolish the possibility that residual importin-α7 still could affect viral replication (Fig. 7). Here, we studied virus RNA accumulation by primer extension analysis in monocycle infections using MEFs isolated from WT or $\alpha7^{-/-}$ mice (12). Adaptive mutations increased vRNA levels in WT and $\alpha7^{-/-}$ cells (Fig. 7A and B). Specifically, vRNA accumulation was increased 220.7% in MEF-$\alpha7^{-/-}$ cells and 2,360.9% in MEF-WT cells. However, importin-α7 dependency persisted with all recombinant viruses analyzed. Accordingly, vRNA accumulation was remarkably reduced during infection of MEF-$\alpha7^{-/-}$ compared to that with MEF-WT cells (Fig. 7C). These data show that importin-α7 dependency remains upon adaptation to $\alpha7^{-/-}$ mice. However, cir-

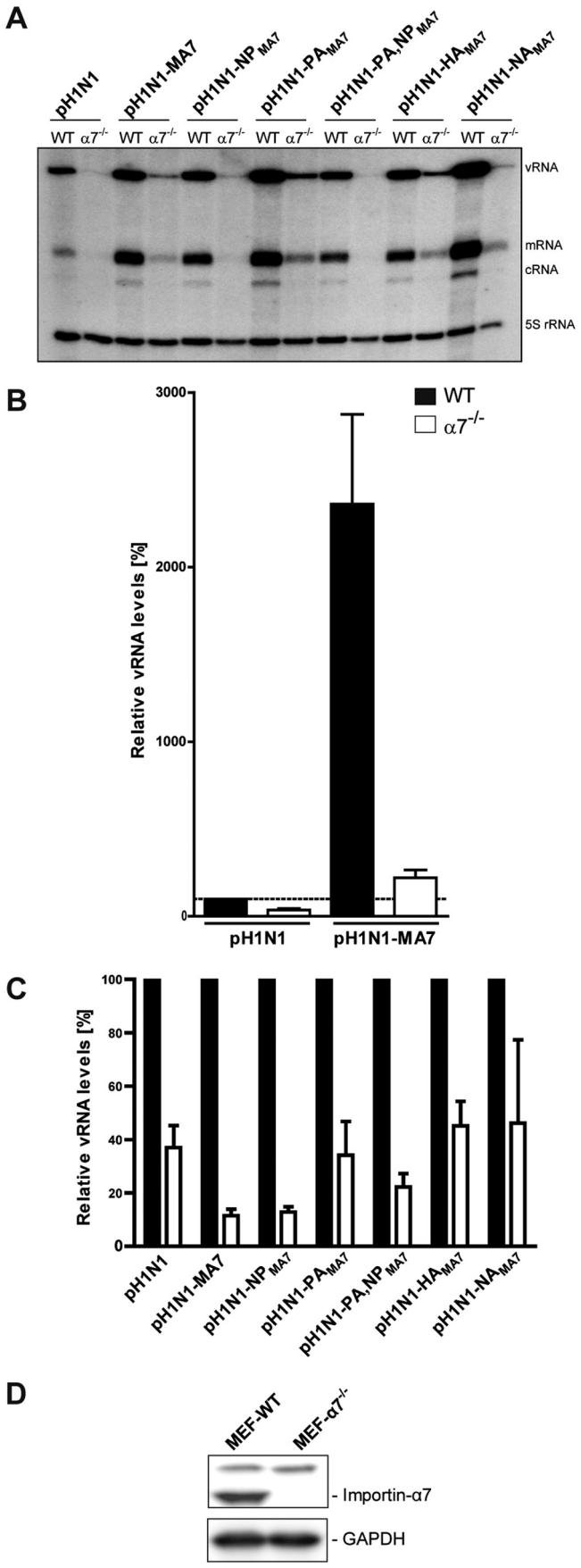

cumvention of the importin-α7 requirement seems to occur by an alternative pathway that results in increased replicative fitness.

DISCUSSION

Antiviral drugs play a key role in mitigating influenza disease severity (27), since most of the circulating influenza virus strains are becoming increasingly resistant against currently available drugs that are directed against viral proteins. Thus, the development of novel antiviral strategies is fundamental (28). Targeting cellular proteins required for viral replication is considered a promising strategy, since cellular proteins generally are less prone to mutations than viral proteins (3).

Here, host factors that are essential for viral infection but not for cellular viability are considered excellent targets for therapeutic intervention (3). In this study, we have chosen importin-α7, which is crucial for human-type influenza virus replication as well as severe lung damage and virulence in mice (7, 9, 16). Most importantly, adult mice lacking the importin-α7 gene appear healthy (8, 10). Thus, this is a particularly attractive factor for transient inhibition to combat acute influenza virus infection. Additionally, recent reports highlight that importin-α belongs to the few host proteins that possess sufficient interactive surface area for virtual screening and host-directed drug discovery (3).

Moreover, antiviral compounds targeting importin-α proteins might comprise a novel panviral strategy to combat various viral infections, since different importin-α isoforms were reported to be utilized by many other viruses, such as hepatitis C virus, HIV, severe acute respiratory syndrome coronavirus, Ebola virus, and dengue virus (29–38). However, developing and evaluating novel antiviral candidates often is time and money consuming. Therefore, we sought to study the feasibility of importin-α7 as an attractive cellular target to combat pandemic influenza virus using an *in vivo* model. Here, we infected $\alpha7^{-/-}$ mice with a 2009 pH1N1 influenza virus and challenged for potential viral escape by serial lung-to-lung passages. Surprisingly, only five passages were required until 100% lethality was reached in $\alpha7^{-/-}$ mice. Importantly, pH1N1-MA7 became approximately 10 times more virulent during viral escape in $\alpha7^{-/-}$ mice than the parental virus strain in WT animals. In contrast, viral variants that escape antiviral drugs, such as oseltamivir, were reported to be as virulent as, but not more virulent than, the parental strain in mice (39). This finding calls for particular caution, since it shows that viral escape can easily occur and leads to the emergence of potentially more virulent strains. This is not in line with previous reports, where viral resistance could not be observed against cellular targets de-

FIG 7 Viral RNA accumulation in WT and $\alpha7^{-/-}$ MEFs infected with pH1N1-MA7 virus. (A) WT and $\alpha7^{-/-}$ MEFs were infected at an MOI of 2 with parental (pH1N1), adapted (pH1N1-MA7), or SGR (pH1N1-PA_{MA7}, pH1N1-NP_{MA7}, pH1N1-PA,NP_{MA7}, pH1N1-HA_{MA7}, and pH1N1-NA_{MA7}) viruses. After 24 h, total RNA was isolated and analyzed by NP gene-specific primer extension. A primer specific for 5S rRNA was used for normalization. (B) vRNA accumulation in MEF-WT (black bars) and MEF-$\alpha7^{-/-}$ (white bars) infected with the parental and adapted viruses. Values were expressed relative to vRNA levels in MEF-WT infected with pH1N1 virus, which was set to 100%. (C) vRNA accumulation was expressed relative to vRNA levels in MEF-WT, which was set to 100% for every virus tested. Data shown represent means ± SEM ($n = 9$ to 12). (D) Importin-α7 expression in MEF cells was checked by Western blotting. Since importin-α7 antibody cross-reacts with importin-α5, the doublet represents importin-α5 (upper band) and importin-α7 (lower band). GAPDH was used as a loading control.

spite serial passaging in cell culture (40). Indeed, no resistance was observed when using the cellular MEK kinase as a target to inhibit influenza B virus replication. However, it should be noted that these studies were performed in cell culture experiments. Since influenza viruses infect several cell types besides epithelial cells, one can speculate that at least the number of cell types to produce potentially more virus variants *in vivo* would be higher than that in cell culture experiments. Moreover, some influenza virus infections may lead to suppression of innate and adaptive immune responses that might further facilitate the emergence of novel virus variants. As stated above, the different selective pressures in cell culture and the whole organism highlight the need for an adequate animal model to evaluate the risk from newly emerging host-targeting drug-resistant virus strains.

Interestingly, escape from importin-α7 requirement was mediated mainly by mutations in the RNP proteins. Thus, weight loss in $\alpha7^{-/-}$ mice was observed only upon infection with recombinant viruses containing NP_{MA7} mutation and was further enhanced when combined with PA_{MA7} mutation. However, combination with adaptive HA and NA mutations was required for an entire circumvention of importin-α7 requirement. However, we did not test the single surface protein mutations combined with vRNP adaptive sites which might have been sufficient for lethality in mice. Thus, several adaptive pathways may have been utilized by the surface glycoproteins and the RNP to overcome the lack of importin-α7.

The PA subunit possesses endonuclease activity that plays a key role in the cap snatching that is required to initiate viral transcription. The PA-D27E mutation is located in the endonuclease domain but outside the active site (22, 41). Hence, this mutation could indirectly influence its endonuclease activity. The NP-G102R mutation is located opposite the oligomerization loop (42, 43). Moreover, the NP-G102R mutant showed a generally reduced binding affinity to other importin-α isoforms relevant for influenza virus replication and pathogenicity (8). This suggests that an alternative nuclear import pathway is preferred, such as the nonclassical nuclear import pathway that is independent of importin-α, like RanBP5, shown to be utilized by PB1 and PA (44). Future studies are required to analyze whether these RNP adaptive mutations represent adaptation to alternative nuclear import pathways or are representative of novel binding sites to viral or cellular proteins increasing virus replication.

Since full circumvention from importin-α7 requirement could be achieved only in combination of adaptive mutations in the RNP with those in HA and NA, drugs targeting crucial host factors might be combined with those preventing cell entry, as shown recently for SALPs (45), or with NA inhibitors, such as oseltamivir, inhibiting viral release to further reduce the risk of antiviral resistance. However, it should be noted that in this case, five mutations in four different gene segments were required to achieve resistance. This could be considered a rather higher resistance barrier compared to that of the single mutation in NA, NA-H274Y, that is sufficient to confer resistance to neuraminidase inhibitors (46). However, the fact that only five passages *in vivo* were sufficient to overcome importin-α7 requirement seems to be rather low. Clearly, future studies will be required to compare the selective pressures required *in vitro* and *in vivo* to overcome drug resistance.

The NA-Y170H mutation that occurred in this study is located in the inner part of the NA tetramer; thus, it is outside the active site of the enzyme (47). This mutation could affect the assembly of NA into tetramers. The receptor binding site (RBS) of HA constitutes three main structural elements: the 190-helix, the 220-loop, and the 130-loop (48). While the HA-K171E mutation is located near the HA RBS, the HA-D239G mutation is included in the 220-loop. Moreover, the D239G substitution corresponds to D222G mutation (H1 numbering) that has been associated with altered receptor specificity, as observed in severe cases of 2009 pandemic H1N1 influenza virus infections in humans (49, 50). As a result, these HA mutations might facilitate receptor binding, thereby increasing virulence in mice.

It should be noted that despite the successful circumvention of the importin-α7 requirement, the pH1N1-MA7 virus still showed dependency, suggesting that the alternative pathway is not entirely able to compensate for the absence of importin-α7. This further highlights that importin-α7 still represents a strong target, but viral escape nevertheless is rapidly possible if only one cellular target is chosen. Thus, future strategies should be directed toward targeting multiple viral and/or cellular factors to reduce the risk of antiviral resistance. This is even more important considering the fact that escape variants from host factors might even be more virulent, posing an increased risk for public health.

ACKNOWLEDGMENTS

This work was supported by grants from the European Union (FLUPHARM) (to G.G.), the Emmy-Noether Programme of the German Research Foundation (to G.G.) (GA 1575/1-1), the Medical Research Council (MRC) (to E.F.) (MR/K000241/1), and the Spanish Ministry of Science and Innovation (MICINN) (to B.O.) (FEDER BIO2011-22568 and EUI2009-04018). P.R.-I. was funded by the Alexander von Humboldt Foundation (3.3SPA/1142463 STP-2) and with a Boehringer Ingelheim Fonds travel grant (BIF TG Infante). D.P. was supported by a Polonsky Foundation Scholarship and Lincoln College, University of Oxford. J.B. was supported by a MICINN fellowship (FEDER BIO2008-0205). The Heinrich-Pette-Institute, Leibniz Institute for Experimental Virology, is supported by the Free and Hanseatic City of Hamburg and the Federal Ministry of Health.

The funders had no role in study design, data collection and analysis, decision to publish, or preparation of the manuscript.

We thank Gökhan Arman-Kalcek and Ilara Hudjetz for excellent technical assistance.

REFERENCES

1. **McCullers JA.** 2005. Antiviral therapy of influenza. Expert Opin Investig Drugs **14:**305–312. http://dx.doi.org/10.1517/13543784.14.3.305.
2. **Ison MG.** 2011. Antivirals and resistance: influenza virus. Curr Opin Virol **1:**563–573. http://dx.doi.org/10.1016/j.coviro.2011.09.002.
3. **Muller KH, Kakkola L, Nagaraj AS, Cheltsov AV, Anastasina M, Kainov DE.** 2012. Emerging cellular targets for influenza antiviral agents. Trends Pharmacol Sci **33:**89–99. http://dx.doi.org/10.1016/j.tips.2011.10.004.
4. **Ludwig S, Zell R, Schwemmle M, Herold S.** 2014. Influenza, a One Health paradigm–novel therapeutic strategies to fight a zoonotic pathogen with pandemic potential. Int J Med Microbiol **304:**894–901. http://dx.doi.org/10.1016/j.ijmm.2014.08.016.
5. **Shaw ML.** 2011. The host interactome of influenza virus presents new potential targets for antiviral drugs. Rev Med Virol **21:**358–369. http://dx.doi.org/10.1002/rmv.703.
6. **Planz O.** 2013. Development of cellular signaling pathway inhibitors as new antivirals against influenza. Antiviral Res **98:**457–468. http://dx.doi.org/10.1016/j.antiviral.2013.04.008.
7. **Hudjetz B, Gabriel G.** 2012. Human-like PB2 627K influenza virus polymerase activity is regulated by importin-alpha1 and -alpha7. PLoS Pathog **8:**e1002488. http://dx.doi.org/10.1371/journal.ppat.1002488.
8. **Gabriel G, Klingel K, Otte A, Thiele S, Hudjetz B, Arman-Kalcek G, Sauter M, Shmidt T, Rother F, Baumgarte S, Keiner B, Hartmann E, Bader M,**

Brownlee GG, Fodor E, Klenk HD. 2011. Differential use of importin-alpha isoforms governs cell tropism and host adaptation of influenza virus. Nat Commun **2:**156. http://dx.doi.org/10.1038/ncomms1158.

9. **Resa-Infante P, Thieme R, Ernst T, Arck PC, Ittrich H, Reimer R, Gabriel G.** 2014. Importin-alpha7 is required for enhanced influenza A virus replication in the alveolar epithelium and severe lung damage in mice. J Virol **88:**8166–8179. http://dx.doi.org/10.1128/JVI.00270-14.
10. **Rother F, Shmidt T, Popova E, Krivokharchenko A, Hugel S, Vilianovich L, Ridders M, Tenner K, Alenina N, Kohler M, Hartmann E, Bader M.** 2011. Importin alpha7 is essential for zygotic genome activation and early mouse development. PLoS One **6:**e18310. http://dx.doi.org/10.1371/journal.pone.0018310.
11. **Reed LJ, Muench H.** 1938. A simple method of estimating fifty percent endpoints. Am J Epidemiol **27:**493–497.
12. **Huegel S, Depping R, Dittmar G, Rother F, Cabot R, Sury MD, Hartmann E, Bader M.** 2014. Identification of importin alpha 7 specific transport cargoes using a proteomic screening approach. Mol Cell Proteomics **13:**1286–1298. http://dx.doi.org/10.1074/mcp.M112.026856.
13. **Otte A, Gabriel G.** 2011. 2009 Pandemic H1N1 influenza A virus strains display differential pathogenicity in C57BL/6J but not BALB/c mice. Virulence **2:**563–566. http://dx.doi.org/10.4161/viru.2.6.18148.
14. **Otte A, Sauter M, Alleva L, Baumgarte S, Klingel K, Gabriel G.** 2011. Differential host determinants contribute to the pathogenesis of 2009 pandemic H1N1 and human H5N1 influenza A viruses in experimental mouse models. Am J Pathol **179:**230–239. http://dx.doi.org/10.1016/j.ajpath.2011.03.041.
15. **Stech J, Stech O, Herwig A, Altmeppen H, Hundt J, Gohrbandt S, Kreibich A, Weber S, Klenk HD, Mettenleiter TC.** 2008. Rapid and reliable universal cloning of influenza A virus genes by target-primed plasmid amplification. Nucleic Acids Res **36:**e139. http://dx.doi.org/10.1093/nar/gkn646.
16. **Gabriel G, Dauber B, Wolff T, Planz O, Klenk HD, Stech J.** 2005. The viral polymerase mediates adaptation of an avian influenza virus to a mammalian host. Proc Natl Acad Sci U S A **102:**18590–18595. http://dx.doi.org/10.1073/pnas.0507415102.
17. **Gabriel G, Herwig A, Klenk HD.** 2008. Interaction of polymerase subunit PB2 and NP with importin alpha1 is a determinant of host range of influenza A virus. PLoS Pathog **4:**e11. http://dx.doi.org/10.1371/journal.ppat.0040011.
18. **Robb NC, Smith M, Vreede FT, Fodor E.** 2009. NS2/NEP protein regulates transcription and replication of the influenza virus RNA genome. J Gen Virol **90:**1398–1407. http://dx.doi.org/10.1099/vir.0.009639-0.
19. **Berman HM, Westbrook J, Feng Z, Gilliland G, Bhat TN, Weissig H, Shindyalov IN, Bourne PE.** 2000. The Protein Data Bank. Nucleic Acids Res **28:**235–242. http://dx.doi.org/10.1093/nar/28.1.235.
20. **Oliva B, Planas-Iglesias J, Bonet J, Marín-López MA, Feliu E, Gursoy A.** 30 March 2012. Structural bioinformatics of proteins: predicting the tertiary and quaternary structure of proteins from sequence, protein-protein interactions. Comput Exp Tools http://dx.doi.org/10.5772/37856.
21. **Altschul SF, Madden TL, Schaffer AA, Zhang J, Zhang Z, Miller W, Lipman DJ.** 1997. Gapped BLAST and PSI-BLAST: a new generation of protein database search programs. Nucleic Acids Res **25:**3389–3402. http://dx.doi.org/10.1093/nar/25.17.3389.
22. **Kowalinski E, Zubieta C, Wolkerstorfer A, Szolar OH, Ruigrok RW, Cusack S.** 2012. Structural analysis of specific metal chelating inhibitor binding to the endonuclease domain of influenza pH1N1 (2009) polymerase. PLoS Pathog **8:**e1002831. http://dx.doi.org/10.1371/journal.ppat.1002831.
23. **van der Vries E, Collins PJ, Vachieri SG, Xiong X, Liu J, Walker PA, Haire LF, Hay AJ, Schutten M, Osterhaus AD, Martin SR, Boucher CA, Skehel JJ, Gamblin SJ.** 2012. H1N1 2009 pandemic influenza virus: resistance of the I223R neuraminidase mutant explained by kinetic and structural analysis. PLoS Pathog **8:**e1002914. http://dx.doi.org/10.1371/journal.ppat.1002914.
24. **Liu J, Stevens DJ, Haire LF, Walker PA, Coombs PJ, Russell RJ, Gamblin SJ, Skehel JJ.** 2009. Structures of receptor complexes formed by hemagglutinins from the Asian influenza pandemic of 1957. Proc Natl Acad Sci U S A **106:**17175–17180. http://dx.doi.org/10.1073/pnas.0906849106.
25. **Fiser A, Sali A.** 2003. Modeller: generation and refinement of homology-based protein structure models. Methods Enzymol **374:**461–491.
26. **Melo F, Feytmans E.** 1998. Assessing protein structures with a non-local atomic interaction energy. J Mol Biol **277:**1141–1152. http://dx.doi.org/10.1006/jmbi.1998.1665.
27. **Ferguson NM, Cummings DA, Fraser C, Cajka JC, Cooley PC, Burke DS.** 2006. Strategies for mitigating an influenza pandemic. Nature **442:**448–452. http://dx.doi.org/10.1038/nature04795.
28. **Govorkova EA, McCullers JA.** 2013. Therapeutics against influenza. Curr Top Microbiol Immunol **370:**273–300.
29. **Frieman M, Yount B, Heise M, Kopecky-Bromberg SA, Palese P, Baric RS.** 2007. Severe acute respiratory syndrome coronavirus ORF6 antagonizes STAT1 function by sequestering nuclear import factors on the rough endoplasmic reticulum/Golgi membrane. J Virol **81:**9812–9824. http://dx.doi.org/10.1128/JVI.01012-07.
30. **Kobiler O, Drayman N, Butin-Israeli V, Oppenheim A.** 2012. Virus strategies for passing the nuclear envelope barrier. Nucleus **3:**526–539. http://dx.doi.org/10.4161/nucl.21979.
31. **Labokha AA, Fassati A.** 2013. Viruses challenge selectivity barrier of nuclear pores. Viruses **5:**2410–2423. http://dx.doi.org/10.3390/v5102410.
32. **Neufeldt CJ, Joyce MA, Levin A, Steenbergen RH, Pang D, Shields J, Tyrrell DL, Wozniak RW.** 2013. Hepatitis C virus-induced cytoplasmic organelles use the nuclear transport machinery to establish an environment conducive to virus replication. PLoS Pathog **9:**e1003744. http://dx.doi.org/10.1371/journal.ppat.1003744.
33. **Pryor MJ, Rawlinson SM, Butcher RE, Barton CL, Waterhouse TA, Vasudevan SG, Bardin PG, Wright PJ, Jans DA, Davidson AD.** 2007. Nuclear localization of dengue virus nonstructural protein 5 through its importin alpha/beta-recognized nuclear localization sequences is integral to viral infection. Traffic **8:**795–807. http://dx.doi.org/10.1111/j.1600-0854.2007.00579.x.
34. **Ramanan P, Shabman RS, Brown CS, Amarasinghe GK, Basler CF, Leung DW.** 2011. Filoviral immune evasion mechanisms. Viruses **3:**1634–1649. http://dx.doi.org/10.3390/v3091634.
35. **Xu W, Edwards MR, Borek DM, Feagins AR, Mittal A, Alinger JB, Berry KN, Yen B, Hamilton J, Brett TJ, Pappu RV, Leung DW, Basler CF, Amarasinghe GK.** 2014. Ebola virus VP24 targets a unique NLS binding site on karyopherin alpha 5 to selectively compete with nuclear import of phosphorylated STAT1. Cell Host Microbe **16:**187–200. http://dx.doi.org/10.1016/j.chom.2014.07.008.
36. **Resa-Infante P, Gabriel G.** 2013. The nuclear import machinery is a determinant of influenza virus host adaptation. Bioessays **35:**23–27. http://dx.doi.org/10.1002/bies.201200138.
37. **Caly L, Wagstaff KM, Jans DA.** 2012. Nuclear trafficking of proteins from RNA viruses: potential target for antivirals? Antiviral Res **95:**202–206. http://dx.doi.org/10.1016/j.antiviral.2012.06.008.
38. **Oksayan S, Ito N, Moseley G, Blondel D.** 2012. Subcellular trafficking in rhabdovirus infection and immune evasion: a novel target for therapeutics. Infect Disord Drug Targets **12:**38–58. http://dx.doi.org/10.2174/187152612798994966.
39. **Hamelin ME, Baz M, Abed Y, Couture C, Joubert P, Beaulieu E, Bellerose N, Plante M, Mallett C, Schumer G, Kobinger GP, Boivin G.** 2010. Oseltamivir-resistant pandemic A/H1N1 virus is as virulent as its wild-type counterpart in mice and ferrets. PLoS Pathog **6:**e1001015. http://dx.doi.org/10.1371/journal.ppat.1001015.
40. **Ludwig S, Wolff T, Ehrhardt C, Wurzer WJ, Reinhardt J, Planz O, Pleschka S.** 2004. MEK inhibition impairs influenza B virus propagation without emergence of resistant variants. FEBS Lett **561:**37–43. http://dx.doi.org/10.1016/S0014-5793(04)00108-5.
41. **Pflug A, Guilligay D, Reich S, Cusack S.** 2014. Structure of influenza A polymerase bound to the viral RNA promoter. Nature **516:**355–360. http://dx.doi.org/10.1038/nature14008.
42. **Ye Q, Krug RM, Tao YJ.** 2006. The mechanism by which influenza A virus nucleoprotein forms oligomers and binds RNA. Nature **444:**1078–1082. http://dx.doi.org/10.1038/nature05379.
43. **Ng AK, Zhang H, Tan K, Li Z, Liu JH, Chan PK, Li SM, Chan WY, Au SW, Joachimiak A, Walz T, Wang JH, Shaw PC.** 2008. Structure of the influenza virus A H5N1 nucleoprotein: implications for RNA binding, oligomerization, and vaccine design. FASEB J **22:**3638–3647. http://dx.doi.org/10.1096/fj.08-112110.
44. **Deng T, Engelhardt OG, Thomas B, Akoulitchev AV, Brownlee GG, Fodor E.** 2006. The role of Ran binding protein 5 (RanBP5) in the nuclear import and assembly of the influenza virus RNA polymerase complex. J Virol **80:**11911–11919. http://dx.doi.org/10.1128/JVI.01565-06.
45. **Hoffmann J, Schneider C, Heinbockel L, Brandenburg K, Reimer R, Gabriel G.** 2014. A new class of synthetic anti-lipopolysaccharide peptides

inhibits influenza A virus replication by blocking cellular attachment. Antiviral Res **104:**23–33. http://dx.doi.org/10.1016/j.antiviral.2014.01.015.
46. **Gubareva LV, Trujillo AA, Okomo-Adhiambo M, Mishin VP, Deyde VM, Sleeman K, Nguyen HT, Sheu TG, Garten RJ, Shaw MW, Fry AM, Klimov AI.** 2010. Comprehensive assessment of 2009 pandemic influenza A (H1N1) virus drug susceptibility in vitro. Antivir Ther **15:**1151–1159. http://dx.doi.org/10.3851/IMP1678.
47. **Varghese JN, Laver WG, Colman PM.** 1983. Structure of the influenza virus glycoprotein antigen neuraminidase at 2.9 A resolution. Nature **303:** 35–40. http://dx.doi.org/10.1038/303035a0.
48. **Yang H, Carney P, Stevens J.** 2010. Structure and receptor binding properties of a pandemic H1N1 virus hemagglutinin. PLoS Curr **2:**RRN1152.
49. **Rykkvin R, Kilander A, Dudman SG, Hungnes O.** 2013. Within-patient emergence of the influenza A(H1N1)pdm09 HA1 222G variant and clear association with severe disease, Norway. Euro Surveill **18:**20369.
50. **Kilander A, Rykkvin R, Dudman SG, Hungnes O.** 2010. Observed association between the HA1 mutation D222G in the 2009 pandemic influenza A(H1N1) virus and severe clinical outcome, Norway 2009-2010. Euro Surveill **15:**19498.